The Chromo-Weibel Instability

Michael Strickland
Frankfurt Institute for Advanced Studies, Johann Wolfgang Goethe - Universität Frankfurt, Max-von-Laue-Straße 1, D-60438 Frankfurt am Main, Germany

Received on 3 December, 2006

I discuss the physics of non-Abelian plasmas which are locally anisotropic in momentum space. Such momentum-space anisotropies are generated by the rapid longitudinal expansion of the matter created in the first 1 fm/c of an ultrarelativistic heavy ion collision. In contrast to locally isotropic plasmas anisotropic plasmas have a spectrum of soft unstable modes which are characterized by exponential growth of transverse chromo-magnetic/-electric fields at short times. This instability is the QCD analogue of the Weibel instability of QED. Parametrically the chromo-Weibel instability provides the fastest method for generation of soft background fields and dominates the short-time dynamics of the system. The existence of the chromo-Weibel instability has been proven using diagrammatic methods, transport theory, and numerical solution of classical Yang-Mills fields. I review the results obtained from each of these methods and discuss the numerical techniques which are being used to determine the late-time behavior of plasmas subject to a chromo-Weibel instability.

Keywords: Quark-Gluon Plasma; Non-Equilibrium Physics; Plasma Instability; Thermalization; Isotropization

I. INTRODUCTION

With the ongoing ultrarelativistic heavy-ion collision experiments at the Relativistic Heavy-Ion Collider (RHIC) and planned the Large Hadron Collider (LHC) physicists hope to produce and study the properties of a thermalized quark-gluon plasma (QGP) which is expected to be formed when the temperature of nuclear matter is raised above its critical value, $T_c \sim 200$ MeV $\sim 10^{12}$ K. Given the small size and short lifetime of the matter created in an ultrarelativistic heavy-ion collision this is not trivially accomplished. One of the chief obstacles to thermalization in ultrarelativistic heavy-ion collisions is the rapid longitudinal expansion of the matter created in the central rapidity region. If the matter expands too quickly then there will not be sufficient time for its constituents to interact and thermalize. During the first 1 fm/c after the nuclear impact the longitudinal expansion causes the created matter to become much colder in the longitudinal direction than in the transverse directions [1], corresponding to $\langle p_L^2 \rangle \ll \langle p_T^2 \rangle$ in the local rest frame. After this initial period of longitudinal cooling, the expansion slows and one can then ask what are the dominant mechanisms for driving the system towards an isotropic thermal QGP.

The evolution of the partonic matter created during a high-energy nuclear collision was among the questions which the "bottom-up" thermalization scenario [1] attempted to answer. For the first time, it addressed the dynamics of soft modes (fields) with momenta much below Q_s coupled to the hard modes (particles) with momenta on the order of Q_s and above [2–4]. However, it has emerged recently that one of the assumptions made in this model was not correct. The debate centers around the first stage of the bottom-up scenario ($1 \ll Q_s\tau \ll \alpha^{-3/2}$) in which it was assumed that (a) collisions between the high-momentum (or hard) modes were the driving force behind isotropization and that (b) the low-momentum (or soft) fields acted only to screen the electric interaction. In doing so, the bottom-up scenario implicitly assumed that the underlying soft gauge modes behaved the same in an anisotropic plasma as in an isotropic one.

However, to be self-consistent one must determine the collective modes which are relevant for an anisotropic plasma and use those. In the case of gauge theories this turns out to be a qualitative rather than quantitative correction since in anisotropic QCD plasmas the most important collective mode corresponds to an instability to transverse chromo-magnetic field fluctuations [5–8]. This instability is the QCD analogue of the QED *Weibel instability* [5]. Recent works have shown that the presence of the *chromo-Weibel instability* is generic for distributions which possess a momentum-space anisotropy [9–11] and have obtained the full non-Abelian hard-loop (HL) action in the presence of an anisotropy [12]. Another important development has been the demonstration that the chromo-Weibel instability also exists in solutions to pure classical Yang-Mills fields in an expanding geometry [13–15].

Recently there have been significant advances in the understanding of non-Abelian soft-field dynamics in anisotropic plasmas within the HL framework [16–19]. The HL framework is equivalent to the collisionless Vlasov theory of eikonalized hard particles, i.e. the particle trajectories are assumed to be unaffected (up to small-angle scatterings with $\theta \sim g$) by the induced background field. It is strictly applicable only when there is a large scale separation between the soft and hard momentum scales. Even with these simplifying assumptions, HL dynamics for non-Abelian theories is complicated by the presence of non-linear gauge-field interactions.

These non-linear interactions become important when the vector potential amplitude is on the order of $A_{\text{non-Abelian}} \sim p_s = g \sim \sqrt{f_h} p_h$, where p_h is the characteristic momentum of the hard particles, e.g. $p_h \sim Q_s$ for CGC initial conditions, f_h is the angle-averaged occupancy at the hard scale, and p_s is the characteristic soft momentum of the fields ($p_s \sim g\sqrt{f_h} p_h$). In QED there is no such complication and the fields grow exponentially until $A_{\text{Abelian}} \sim p_h/g$ at which point the hard particles undergo large-angle deflections by the soft background field which rapidly isotropize the system. In fact, in QED the Weibel instability is the fastest process driving plasma isotropization. In QCD, however, the effect of the non-linear

gauge self-interactions affects the system's dynamics primarily slowing down instability-driven particle isotropization.

To include the effects of gauge self-interactions numerical studies of the time evolution of the gauge-covariant HL equations of motion are required. Recent numerical studies of HL gauge dynamics for SU(2) gauge theory indicate that for *moderate* anisotropies the gauge field dynamics changes from exponential field growth indicative of a conventional Abelian plasma instability to linear growth when the vector potential amplitude reaches the non-Abelian scale, $A_{\rm non-Abelian} \sim p_{\rm h}$ [17, 18]. This linear growth regime is characterized by a turbulent cascade of the energy pumped into the soft modes by the instability to higher-momentum plasmon-like modes [20, 21]. These results indicate that there is a fundamental difference between Abelian and non-Abelian plasma instabilities in the HL limit.

In addition to numerical studies in the HL limit there have been numerical results from the solution to the full non-linear Vlasov equations for anisotropic plasmas [22, 23]. This approach can be shown to reproduce the HL effective action in the weak-field approximation [24–26]; however, when solved fully the approach goes beyond the HL approximation since the full classical transport theory also reproduces some higher n-point vertices of the dimensionally reduced effective action for static gluons [27]. Numerical solution of the 3d Vlasov equations show that chromo-instabilities persist beyond the HL limit [23]. Furthermore, the soft field spectrum obtained from full Vlasov simulations shows a cascade or "avalanche" of energy deposited in the soft unstable modes in higher momentum modes similar to HL dynamics.

II. ANISOTROPIC GLUON POLARIZATION TENSOR

In this section, I consider a quark-gluon plasma with a parton distribution function which is decomposed as [9]

$$f(\mathbf{p}) \equiv 2N_f\left[n_q(\mathbf{p})+n_{\bar{q}}(\mathbf{p})\right]+4N_c\, n_g(\mathbf{p})\,, \tag{1}$$

where n_q, $n_{\bar{q}}$, and n_g are the distribution functions of quarks, anti-quarks, and gluons, respectively, and the numerical coefficients collect all appropriate symmetry factors. Using the result of Ref. [9] the spacelike components of the HL gluon self-energy for gluons with soft momentum ($k \sim g\, p_{\rm hard}$) can be written as

$$\Pi^{ij}_{ab}(K) = -\frac{g^2}{2}\,\delta_{ab}\int\frac{d^3\mathbf{p}}{(2\pi)^3}v^i\frac{\partial f(\mathbf{p})}{\partial p^l}\left(\delta^{jl}+\frac{v^jk^l}{K\cdot V+i\varepsilon}\right)\,, \tag{2}$$

where $K=(\omega,\mathbf{k})$, $V=(1,\mathbf{p}/p)$, and the parton distribution function $f(\mathbf{p})$ is, up to an integrability requirement, completely arbitrary. In what follows we will assume that $f(\mathbf{p})$ can be obtained from an isotropic distribution function by the rescaling of only one direction in momentum space.

In practice this means that, given any isotropic parton distribution function $f_{\rm iso}(p)$, we can construct an anisotropic version by changing the argument of the isotropic distribution function, $f(\mathbf{p}) = f_{\rm iso}\left(\sqrt{\mathbf{p}^2+\xi(\mathbf{p}\cdot\hat{\mathbf{n}})^2}\right)$, where $\hat{\mathbf{n}}$ is the direction of the anisotropy, and $\xi > -1$ is an adjustable anisotropy parameter with $\xi = 0$ corresponding to the isotropic case. Here we will concentrate on $\xi > 0$ which corresponds to a contraction of the distribution along the $\hat{\mathbf{n}}$ direction since this is the configuration relevant for heavy-ion collisions at early times, namely two hot transverse directions and one cold longitudinal direction.

Making a change of variables in (2) it is possible to integrate out the $|p|$-dependence giving [9]

$$\Pi^{ij}_{ab}(\omega/k,\theta_n) \;=\; m_D^2\,\delta_{ab}\int\frac{d\Omega}{4\pi}v^i\frac{v^l+\xi(\mathbf{v}\cdot\hat{\mathbf{n}})\hat{n}^l}{(1+\xi(\mathbf{v}\cdot\hat{\mathbf{n}})^2)^2} \times\left(\delta^{jl}+\frac{v^jk^l}{K\cdot V+i\varepsilon}\right), \tag{3}$$

where $\cos\theta_n \equiv \hat{\mathbf{k}}\cdot\hat{\mathbf{n}}$ and $m_D^2 > 0$. The isotropic Debye mass, m_D, depends on $f_{\rm iso}$ but is parametrically $m_D \sim g\, p_{\rm hard}$.

The next task is to construct a tensor basis for the spacelike components of the gluon self-energy and propagator. We therefore need a basis for symmetric 3-tensors which depend on a fixed anisotropy 3-vector $\hat{n}^i$ with $\hat{n}^2 = 1$. This can be achieved with the following four component tensor basis: $A^{ij} = \delta^{ij} - k^ik^j/k^2$, $B^{ij} = k^ik^j/k^2$, $C^{ij} = \tilde{n}^i\tilde{n}^j/\tilde{n}^2$, and $D^{ij} = k^i\tilde{n}^j + k^j\tilde{n}^i$ with $\tilde{n}^i \equiv A^{ij}\hat{n}^j$. Using this basis we can decompose the self-energy into four structure functions α, β, γ, and δ as $\Pi = \alpha\mathbf{A}+\beta\mathbf{B}+\gamma\mathbf{C}+\delta\mathbf{D}$. Integral expressions for α, β, γ, and δ can be found in Ref. [9] and [11].

III. COLLECTIVE MODES

As shown in Ref. [9] this tensor basis allows us to express the propagator in terms of the following three functions

$$\begin{aligned}\Delta_\alpha^{-1}(K) &= k^2-\omega^2+\alpha\,,\\ \Delta_\pm^{-1}(K) &= \omega^2-\Omega_\pm^2\,,\end{aligned}$$

where $2\Omega_\pm^2 = \bar{\Omega}^2 \pm \left(\bar{\Omega}^4 - 4((\alpha+\gamma+k^2)\beta - k^2\tilde{n}^2\delta^2)\right)^{1/2}$ and $\bar{\Omega}^2 = \alpha+\beta+\gamma+k^2$.

Taking the static limit of these three propagators we find that there are three mass scales: $m_\pm$ and m_α. In the isotropic limit, $\xi\to 0$, $m_\alpha^2 = m_-^2 = 0$ and $m_+^2 = m_D^2$. However, for $\xi > 0$ we find that $m_\alpha^2 < 0$ for all $|\theta_n| \neq \pi/2$ and $m_-^2 < 0$ for all $|\theta_n| \leq \pi/4$. Note also that for $\xi > 0$ both m_α^2 and m_-^2 have there largest negative values at $\theta_n = 0$ where they are equal.

The fact that for $\xi > 0$ both m_α^2 and m_-^2 can be negative indicates that the system is unstable to both magnetic and electric fluctuations with the fastest growing modes focused along the beam line ($\theta_n = 0$). In fact it can be shown that there are two purely imaginary solutions to each of the dispersion relations $\Delta_\alpha^{-1}(K) = 0$ and $\Delta_-^{-1}(K) = 0$ with the solutions in the upper half plane corresponding to unstable modes. We can determine the growth rate for these unstable modes by taking $\omega \to i\Gamma$ and then solving the resulting dispersion relations for $\Gamma(k)$. Typical dispersion relations are shown in Fig. 1.

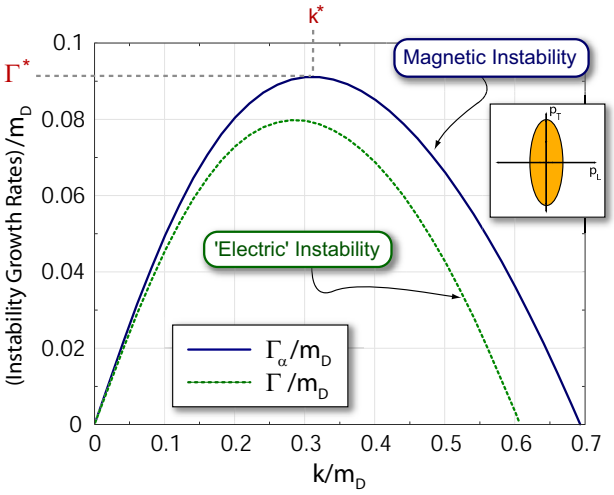

FIG. 1: Instability growth rates as a function of wave number for $\xi = 10$ and $\theta_n = \pi/8$. Note that both growth rates vanish at $k = 0$ and have a maximum $\Gamma^* \sim m_D/10$ at $k^* \sim m_D/3$. The fact that they have a maximum means that at early times the system will be dominated by unstable modes with spatial frequency $\propto 1/k^*$ which grow at a rate Γ^*.

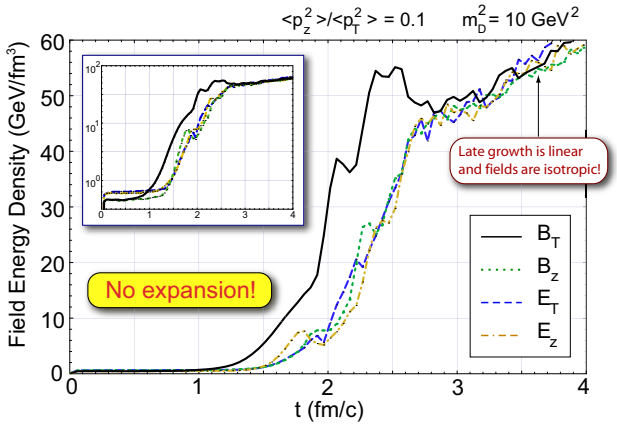

FIG. 2: Plot of typical energy densities observed in non-expanding three-dimensional hard-loop simulation of the soft-fields generated in an anisotropic plasma with $\xi = 10$. Shows transition from exponential growth with preference for transverse magnetic fields to linear isotropic growth. Inset shows same data on logarithmic vertical axis. To obtain physical units we have used $\alpha_s = 0.3$ and $Q_s = 1.5$ GeV.

IV. DISCRETIZED HARD-LOOP DYNAMICS

It is possible to go beyond an analysis of gluon polarization tensor to a full effective field theory for the soft modes and then solve this numerically. The effective field theory for the soft modes that is generated by integrating out the hard plasma modes at one-loop order and in the approximation that the amplitudes of the soft gauge fields obey $A \ll |\mathbf{p}|/g$ is that of the gauge-covariant collisionless Boltzmann-Vlasov equations [28]. In equilibrium, the corresponding (nonlocal) effective action is the so-called hard-thermal-loop effective action which has a simple generalization to plasmas with anisotropic momentum distributions [12]. For the general non-equilibrium situation the resulting equations of motion are

$$\begin{aligned} D_\nu(A)F^{\nu\mu} &= -g^2 \int \frac{d^3p}{(2\pi)^3}\frac{1}{2|\mathbf{p}|}\, p^\mu \frac{\partial f(\mathbf{p})}{\partial p^\beta} W^\beta(x;\mathbf{v})\,, \\ F_{\mu\nu}(A)v^\nu &= [v\cdot D(A)]\, W_\mu(x;\mathbf{v})\,, \end{aligned} \tag{4}$$

where f is a weighted sum of the quark and gluon distribution functions [12] and $v^\mu \equiv p^\mu/|\mathbf{p}| = (1,\mathbf{v})$.

These equations include all hard-loop resummed propagators and vertices and are implicitly gauge covariant. At the expense of introducing a continuous set of auxiliary fields $W_\beta(x;\mathbf{v})$ the effective field equations are also local. These equations of motion are then discretized in space-time and $\mathbf{v}$, and solved numerically. The discretization in $\mathbf{v}$-space corresponds to including only a finite set of the auxiliary fields $W_\beta(x;\mathbf{v}_i)$ with $1 \le i \le N_W$. For details on the precise discretizations used see Refs. [17, 18].

A. Discussion of Hard-Loop Results

During the process of instability growth the soft gauge fields get the energy for their growth from the hard particles and, of course, the total energy is conserved. In an Abelian plasma the energy deposited in soft fields grows exponentially until the energy in the soft fields is of the same order as the energy remaining in the hard particles at which point the back-reaction of the fields on the particle motion causes rapid isotropization. As mentioned above in a non-Abelian plasma the situation is quite different and one must rely on numerical simulations due to the presence of strong gauge field self-interactions.

In Fig. 2, I have plotted the time dependence of the chromo-magnetic/-electric energy densities obtained from a 3+1 dimensional from a typical HL simulation run initialized with "weak" random color noise with $\xi = 10$ [18]. The inset shows the data on a logarithmic scale. As can be seen from this figure at $t \simeq 2.5$ fm/c there is a change from exponential to linear growth. Another interesting feature of the isotropic linear growth phase is that it exhibits a cascade of energy pumped into the unstable soft modes to higher energy plasmon like modes. This is demonstrated in Fig. 3 which shows the soft gauge field spectrum as a function of momentum at different simulation times in the saturated linear regime along with the estimated scaling coefficient of the spectrum [20].

Note, in addition, Ref. [20] showed that there were non-perturbatively large chaotic Chern-Simons number fluctuations in the linear growth phase. This should be contrasted to an Abelian theory or weak-field non-Abelian theory in which Chern-Simons number can fluctuate around zero but does not give large values when it is averaged over time. This is further indication of the non-perturbative physics associated with the chromo-Weibel instability.

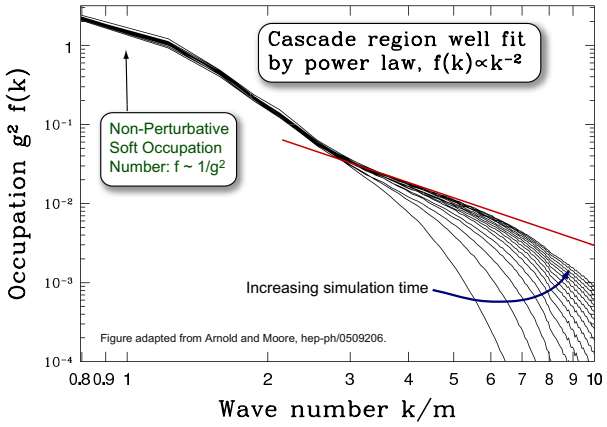

FIG. 3: Field mode spectrum for SU(2) runs showing saturation of soft field growth at $f \sim 1/g^2$ and an associated cascade of energy to the UV as the simulation time increases. Figure adapted from Ref. [20].

From Fig. 2 we can conclude that the chromo-Weibel instability will be less efficient at isotropizing a QCD plasma than the analogous Weibel instability seen in Abelian plasmas due to the slower than exponential growth at late times. On the positive side, from a theoretical perspective "saturation" at the soft scale implies that one can still apply the hard-loop effective theory self-consistently to understand the behavior of the system in the linear growth phase.

One caveat is that the latest published HL simulation results [17, 18] are for distributions with a finite $O(1\to 10)$ anisotropy due to computational limitations and saturation seems to imply that for weak anisotropies field instabilities will not rapidly isotropize the hard particles. This means, however, that due to the continued expansion of the system the anisotropy will increase. It is therefore important to understand the behavior of the system for more extreme anisotropies. More importantly it is necessary to study the hard-loop dynamics in an expanding system. Naively, one expects this to change the growth from $\exp(\tau)$ to $\exp(\sqrt{\tau})$ at short times but there is no clear expectation of what will happen in the linear regime. A significant advance in this regard has occurred recently for a U(1) gauge theory [19]. Work is underway to do the same for non-Abelian gauge theories.

V. WONG-YANG-MILLS EQUATIONS

It is also to possible to go beyond the hard-loop approximation and solve instead the full classical transport equations in three dimensions [23]. The Vlasov transport equation for hard gluons with non-Abelian color charge q^a in the collisionless approximation are [29, 30],

$$p^\mu[\partial_\mu - g q^a F^a_{\mu\nu}\partial^\nu_p - g f_{abc} A^b_\mu q^c \partial_{q^a}] f(x,p,q) = 0\,. \qquad (5)$$

Here, $f(t,\mathbf{x},\mathbf{p},\mathbf{q^a})$ denotes the single-particle phase space distribution function.

The Vlasov equation is coupled self-consistently to the Yang-Mills equation for the soft gluon fields,

$$D_\mu F^{\mu\nu} = J^\nu = g\int \frac{d^3p}{(2\pi)^3} dq\, q\, v^\nu f(t,\mathbf{x},\mathbf{p},\mathbf{q})\,, \qquad (6)$$

with $v^\mu \equiv (1,\mathbf{p}/\mathbf{p})$. These equations reproduce the "hard thermal loop" effective action near equilibrium [24–26]. However, the full classical transport theory, Eqs. (5,6), also reproduces some higher n-point vertices of the dimensionally reduced effective action for static gluons [27] beyond the hard-loop approximation. The back-reaction of the long-wavelength fields on the hard particles ("bending" of their trajectories) is, of course, taken into account, which is important for understanding particle dynamics in strong fields.

Eq. (5) can be solved numerically by replacing the continuous single-particle distribution $f(\mathbf{x},\mathbf{p},\mathbf{q})$ by a large number of test particles:

$$f(\mathbf{x},\mathbf{p},\mathbf{q}) = \frac{1}{N_{\rm test}}\sum_i \delta(\mathbf{x}-\mathbf{x_i}(\mathbf{t})) \times (2\pi)^3\delta(\mathbf{p}-\mathbf{p_i}(\mathbf{t}))\,\delta(\mathbf{q^a}-\mathbf{q_i^a}(\mathbf{t}))\,, \qquad (7)$$

where $\mathbf{x_i}(\mathbf{t})$, $\mathbf{p_i}(\mathbf{t})$ and $q_i^a(t)$ are the position, momentum, and color phase-space coordinates of an individual test particle and $N_{\rm test}$ denotes the number of test-particles per physical particle. The *Ansatz* (7) leads to Wong's equations [29, 30]

$$\frac{d\mathbf{x_i}}{dt} = \mathbf{v_i}\,, \qquad (8)$$

$$\frac{d\mathbf{p_i}}{dt} = g\,q_i^a\,(\mathbf{E^a}+\mathbf{v_i}\times\mathbf{B^a})\,, \qquad (9)$$

$$\frac{d\mathbf{q_i}}{dt} = ig\,v_i^\mu[A_\mu,\mathbf{q_i}]\,, \qquad (10)$$

$$J^{a\nu} = \frac{g}{N_{\rm test}}\sum_i q_i^a\, v^\nu\,\delta(\mathbf{x}-\mathbf{x_i}(\mathbf{t}))\,. \qquad (11)$$

for the i-th test particle. The time evolution of the Yang-Mills field can be followed by the standard Hamiltonian method [31] in $A^0 = 0$ gauge. For details of the numerical implementation used see Ref. [23].

In Fig. 4, I present the results of a three-dimensional Wong-Yang-Mills (WYM) simulation published in Ref. [23]. The figure shows the time evolution of the field energy densities for $SU(2)$ gauge group resulting from a highly anisotropic initial particle momentum distribution. The behavior shown in Fig. 4 indicates that the results obtained from the hard-loop simulations and direct numerical solution of the WYM equations are qualitatively similar in that both show that for non-Abelian gauge theories there is a saturation of the energy transferred to the soft modes by the gauge instability. Although I don't show it here the corresponding Coulomb gauge fixed field spectra show that the field saturation is accompanied by an "avalanche" of energy transferred to soft field modes to higher frequency field modes with saturation occurring when the hardest lattice modes are filled [23].

A more thorough analytic understanding of this ultraviolet avalanche is lacking at this point in time although some

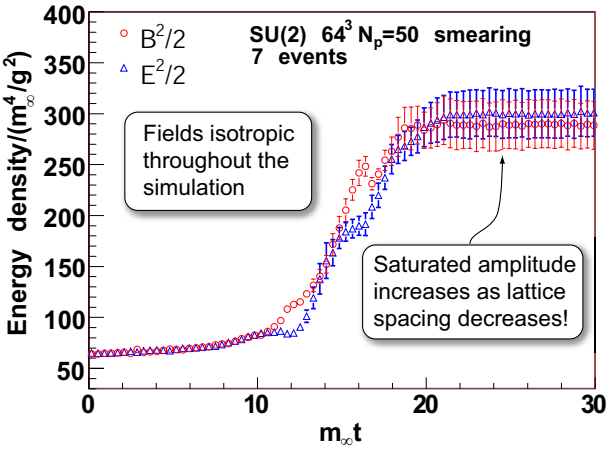

FIG. 4: Time evolution of the field energy densities for $SU(2)$ gauge group resulting from a highly anisotropic initial particle momentum distribution. Simulation parameters are $L = 5$ fm, $p_{\rm hard} = 16$ GeV, $g^2 n_g = 10/\mathrm{fm}^3$, $m_\infty = 0.1$ GeV.

advances in this regard have been made recently [32]. Additionally, since within the numerical solution of the WYM equations the ultraviolet modes become populated rapidly this means that the effective theory which relies on a separation between hard (particle) and soft (field) scales breaks down. This should motivate research into numerical methods which can be used to "shuffle" field modes to particles when their momentum becomes too large and vice-versa for hard particles. Hopefully, using such methods it will be possible to simulate the non-equilibrium dynamics of anisotropic plasmas in a self-consistent numerical framework which treats particles and fields and the transmutation between these two types of degrees of freedom self-consistently.

VI. OUTLOOK

An important open question is whether quark-gluon plasma instabilities and/or the physics of anisotropic plasmas in general play an important phenomenological role at RHIC or LHC energies. In this regard the recent papers of Refs. [33–36] provide theoretical frameworks which can be used to calculate the impact of anisotropic momentum-space distributions on observables such as jet shapes and the rapidity dependence of medium-produced photons. A concrete example of work in this direction is the recent calculation of photon production from an anisotropic QGP [37]. The results of that work suggest that it may be able possible to determine the time-dependent anisotropy of a QGP by measuring the rapidity dependence of high-energy medium photon production.

[1] R. Baier, A. H. Mueller, D. Schiff, and D. T. Son, Phys. Lett. B **502**, 51 (2001), hep-ph/0009237.
[2] A. H. Mueller, Nucl. Phys. A **715**, 20 (2003), hep-ph/0208278.
[3] E. Iancu and R. Venugopalan (2003), hep-ph/0303204.
[4] L. McLerran, Nucl. Phys. A **752**, 355 (2005).
[5] E. Weibel, Phys. Rev. Lett. **2**, 83 (1959).
[6] S. Mrowczynski, Phys. Lett. B **314**, 118 (1993).
[7] S. Mrowczynski, Phys. Rev. C **49**, 2191 (1994).
[8] S. Mrowczynski, Phys.Lett.B**393**, 26(1997),hep-ph/9606442.
[9] P. Romatschke and M. Strickland, Phys. Rev. D **68**, 036004 (2003), hep-ph/0304092.
[10] P. Arnold, J. Lenaghan, and G. D. Moore, JHEP **08**, 002 (2003), hep-ph/0307325.
[11] P. Romatschke and M. Strickland, Phys. Rev. D **70**, 116006 (2004), hep-ph/0406188.
[12] S. Mrowczynski, A. Rebhan, and M. Strickland, Phys. Rev. D **70**, 025004 (2004), hep-ph/0403256.
[13] P. Romatschke and R. Venugopalan (2005), hep-ph/0510292.
[14] P. Romatschke and R. Venugopalan, Phys. Rev. Lett. **96**, 062302 (2006), hep-ph/0510121.
[15] P. Romatschke and R. Venugopalan (2006), hep-ph/0605045.
[16] A. Rebhan, P. Romatschke, and M. Strickland, Phys. Rev. Lett. **94**, 102303 (2005), hep-ph/0412016.
[17] P. Arnold, G. D. Moore, and L. G. Yaffe, Phys. Rev. D **72**, 054003 (2005), hep-ph/0505212.
[18] A. Rebhan, P. Romatschke, and M. Strickland, JHEP **09**, 041 (2005), hep-ph/0505261.
[19] P. Romatschke and A. Rebhan (2006), hep-ph/0605064.
[20] P. Arnold and G. D. Moore, Phys. Rev. D **73**, 025006 (2006), hep-ph/0509206.
[21] P. Arnold and G. D. Moore, Phys. Rev. D **73**, 025013 (2006), hep-ph/0509226.
[22] A. Dumitru and Y. Nara, Phys. Lett. B **621**, 89 (2005), hep-ph/0503121.
[23] A. Dumitru, Y. Nara, and M. Strickland (2006), hep-ph/0604149.
[24] P. F. Kelly, Q. Liu, C. Lucchesi, and C. Manuel, Phys. Rev. Lett. **72**, 3461 (1994), hep-ph/9403403.
[25] P. F. Kelly, Q. Liu, C. Lucchesi, and C. Manuel, Phys. Rev. D **50**, 4209 (1994), hep-ph/9406285.
[26] J.-P. Blaizot and E. Iancu, Nucl. Phys. B **557**, 183 (1999), hep-ph/9903389.
[27] M. Laine and C. Manuel, Phys. Rev. D **65**, 077902 (2002), hep-ph/0111113.
[28] J.-P. Blaizot and E. Iancu, Phys. Rept. **359**, 355 (2002), hep-ph/0101103.
[29] S. K. Wong, Nuovo Cim. A **65**, 689 (1970).
[30] U. W. Heinz, Phys. Rev. Lett. **51**, 351 (1983).
[31] J. Ambjørn, T. Askgaard, H. Porter, and M. E. Shaposhnikov, Nucl. Phys. B **353**, 346 (1991).
[32] A. H. Mueller, A. I. Shoshi, and S. M. H. Wong (2006), hep-ph/0607136.
[33] P. Romatschke and M. Strickland, Phys. Rev. D **69**, 065005 (2004), hep-ph/0309093.
[34] P. Romatschke and M. Strickland, Phys. Rev. D **71**, 125008 (2005), hep-ph/0408275.
[35] B. Schenke and M. Strickland (2006), hep-ph/0606160.
[36] P. Romatschke (2006), hep-ph/0607327.
[37] B. Schenke and M. Strickland (2006), hep-ph/0611332.